Progress in Orthodontics

RESEARCH

Open Access

Embrasure aligner fit and thickness in 3D-printed and thermoformed aligners: a microcomputed tomography study

Ho-Jin Kim[1] and Hyo-Sang Park[1*]

Abstract

Background This study evaluated the fit and thickness of aligners at tooth embrasures, comparing three-dimensional (3D)-printed and thermoformed aligners.

Materials and methods Thirty aligners—3D-printed (no-offset and 0.05 mm offset) and thermoformed—were fabricated and mounted on a maxillary dental model. All aligners were scanned using microcomputed tomography. Embrasure gap distance and thickness were measured at coronal and cervical levels, and ratios reflecting aligner fit and thickness changes after fabrication were calculated. The Kruskal–Wallis and Mann–Whitney U tests were used for group and vertical level comparisons.

Results The 0.05 mm offset 3D-printed aligners exhibited significantly smaller embrasure gaps than the no-offset 3D-printed and thermoformed aligners, with no significant differences between coronal and cervical levels. The other groups showed larger gaps at the cervical level. The embrasure fit ratio was higher in the 0.05 mm offset 3D-printed group (73–93%) compared with the no-offset 3D-printed group (58–86%) and thermoformed group (44–85%). Thermoformed aligners demonstrated significant thickness reduction after fabrication, with ratios of 36.5–88.5% relative to the original sheet, whereas 3D-printed aligners exhibited significant thickness increases, with ratios of 197–470% relative to the virtual design.

Conclusions The 0.05 mm offset 3D-printed aligners exhibited a superior fit compared with the no-offset 3D-printed and thermoformed aligners. The 3D-printed aligners showed significant thickness increases at embrasures, in contrast to the notable thickness reductions observed in thermoformed aligners.

Keywords Embrasure fit, 3D-printed aligners, Thermoformed aligners, Microcomputed tomography

*Correspondence:
Hyo-Sang Park
parkhs@knu.ac.kr
[1]Department of Orthodontics, School of Dentistry, Kyungpook National University, Daegu, Republic of Korea

Background

The use of clear aligners has steadily increased, supported by improvements in the accuracy of tooth movement. While treatment outcomes are more predictable than in the past, discrepancies between virtual treatment plans and clinical results persist, particularly in cases involving rotation, mesiodistal translation, and extrusion [1–3]. A contributing factor may be insufficient aligner grip on the tooth surface [1, 4]. During the thermoforming process, relatively poor fit and reduced thickness may occur, especially in areas with large undercuts created by severe malalignment or pronounced buccolingual tooth inclinations [5–7]. These deficiencies can compromise force application at the cervical areas, increasing unintended intrusion and uncontrolled tipping rather than achieving the intended controlled tipping and bodily movement [8, 9]. To address these limitations, attachments are commonly used to enhance aligner retention and force delivery [1]. However, even with attachments, discrepancies between planned and actual tooth movements persist. Previous studies have reported an accuracy of less than 60% in mesiodistal tipping 1, with the maxillary teeth exhibiting an average loss of 0.4 mm in mesiodistal translation for every 1 mm of planned movement [10].

Improved fit within tooth embrasure areas can increase the aligner–tooth contact surface. A longer contact distance and a broader contact area may generate a greater moment, as intended, thereby improving the precision of tooth movement. Hence, accurate adaptation and optimal thickness in the embrasure region, particularly beneath the interproximal contact point, may be critical in achieving desired tooth movements [11].

Recent advancements in aligner materials have further enhanced adaptation. These include multilayer thermoplastic sheets that combine rigid and elastic layers [12, 13] and three-dimensional (3D) printable materials with shape-memory properties [14]. Such materials might provide better force delivery and facilitate more physiologic tooth movement. However, even with these advanced materials, the clinical performance of clear aligners is still highly dependent on their physical adaptation to the tooth surface and appropriate thickness to ensure adequate orthodontic force. These factors are crucial for the effective transfer of optimal forces generated by sequentially staged aligners [13]. To evaluate these properties non-destructively and with high precision, microcomputed tomography (MicroCT) has been widely used. Although previous research comparing 3D-printed and thermoformed aligners has reported no significant differences in gap distance to the tooth surface [15], most analyses have been limited to buccolingual and occlusal surfaces [5, 16]. Limited research has precisely examined the fit and thickness of aligners in the embrasure regions, despite their potential importance for accurate force and moment application [11].

This study aimed to compare embrasure fit and thickness among 3D-printed aligners designed with and without a 0.05-mm inner surface offset and thermoformed aligners. To further clarify the clinical implications, the ratios of aligner adaptation relative to tooth embrasure depth and aligner thickness relative to the original design set or thermoplastic sheet thickness were also evaluated. The null hypothesis was that no significant differences in embrasure gap or thickness would exist between the aligner groups.

Materials and methods

This study has received approval from the Institutional Review Board of Kyungpook National University Dental Hospital (No.: KNUDH-2025-02-01-00).

A maxillary dental model with an ovoid arch form and a 2-mm tooth size–arch length discrepancy was used. The model exhibited no dental spacing and had tight interproximal contacts, with a mean buccopalatal contact distance of 1.51 ± 0.50 mm. Using an occlusal plane defined by the midpoint of the incisal edges of the central incisors and the mesiobuccal cusp tips of the first molars, the average undercut height and depth were 7.82 ± 1.84 mm and 2.23 ± 0.86 mm for anterior teeth, and 2.28 ± 0.88 mm and 0.55 ± 0.30 mm for the posterior teeth, respectively [17].

The dental model was digitized into a stereolithography (STL) file using an intraoral scanner (Trios 4, 3Shape, Copenhagen, Denmark). The STL file was used to fabricate 3D-printed and thermoformed aligners. Based on a sample size calculation from previously published data [18], 10 samples per group were required to achieve 80% statistical power at a 5% significance level, with an effect size of 1.36. Previous studies have reported an average trueness difference of 0.10–0.40 mm between 3D-printed and thermoformed aligners [15, 19].

3D-printed aligners

The STL file was imported into virtual aligner design software (Direct Aligner Designer, Graphy Inc., Seoul, Korea). Digital aligner models were created with a uniform thickness of 0.5 mm and straight margins placed 1 mm below the cementoenamel junction (CEJ). Two designs differing in inner surface offset, were generated: one without offset and one with a 0.05-mm offset (Fig. 1), based on a previous MicroCT study [20]. Each digital aligner was positioned at a 45° tilt on the build platform. Support structures were automatically generated on the outer occlusal surfaces of the aligners to minimize interference with the internal fit using the aligner design software (Direct Aligner Designer, Graphy Inc., Seoul, Korea). The aligners were printed with a digital

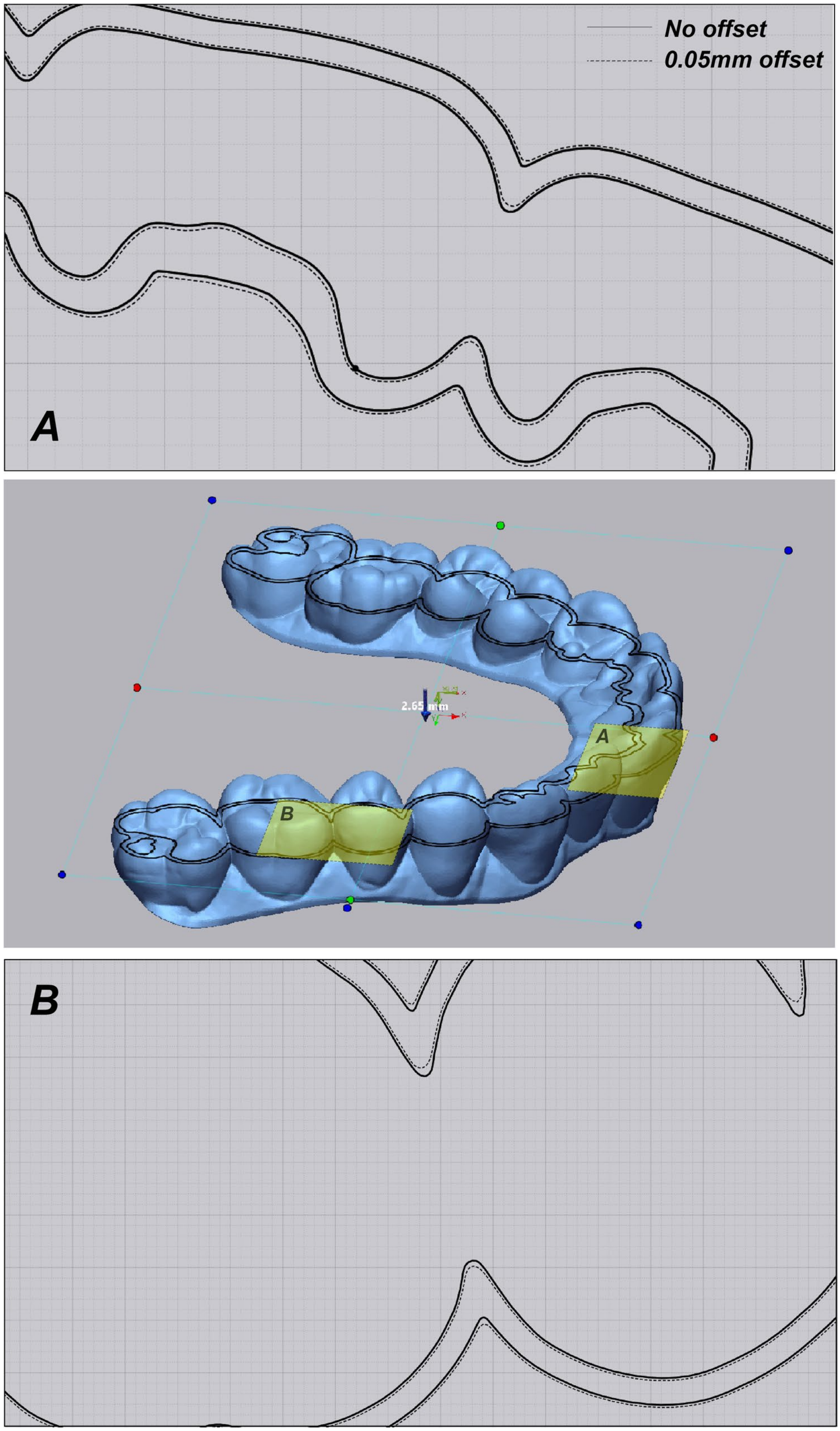

Fig. 1 Virtual design of the 3D-printed aligner and inner surface offset. **A** Axial section of the central and lateral incisors. **B** Axial section of the second premolar and first molar

light processing printer (NBEE, v3.13, Uniz, San Diego, CA, USA) at a 50-μm layer thickness using a clear photocurable resin (TA-28, Graphy Inc., Seoul, Korea; Lot #1-FG07B02069). Post-processing included uncured resin removal by centrifugation at 500 rpm for 6 min, detachment of supports, and ultraviolet curing under a nitrogen atmosphere for 20 min (405 nm light-emitting diodes; Tera Harz Cure, Graphy Inc., Seoul, Korea). To complete polymerization, aligners were immersed in 100 °C water for 1 min, followed by ultrasonic cleaning in 70 °C water for 3 min.

Thermoformed aligners

Ten dental models were printed using the same STL file with a 50-μm layer thickness and a 12-mm base height (S-200 M, Graphy Inc., Seoul, Korea; Lot #1-FH21C07104). The printed models were cleaned with isopropyl alcohol for 1 min, post-cured for 6 min (Tera Harz Cure, Graphy Inc., Seoul, Korea), and ultrasonically cleaned in 70 °C water for 3 min. Thermoformed aligners were fabricated using 0.75 mm x 125 mm three-layer thermoplastic sheets (CA Pro+, Scheu Dental, Iserlohn, Germany). The sheets were heated at 220 °C for 25 s and formed over the dental models (under 4.8 bar of vacuum pressure), followed by 60 s of air cooling (Biostar, Scheu-Dental, Iserlohn, Germany). The aligners were then trimmed 1 mm below the CEJ using a straight cut line, carefully removed from the models, and polished along the margins.

MicroCT scanning and analysis

A total of 30 aligners (no-offset 3D-printed, 0.05-mm offset 3D-printed, and thermoformed) were evaluated. All aligners were mounted onto an identical maxillary model printed from the same STL file used for their fabrication. The 3D-printed aligners were conditioned by immersion in 70 °C water, applied to the model, and dried with warm air at 37 °C before scanning, while the thermoformed aligners were applied at room temperature.

Scanning was performed using a MicroCT scanner (X-eye CT, SEC Co., LTD, Korea) at 154 kVp and 62 mA, with a voxel resolution of 40 μm. Image reconstruction was performed using standard convolution and back-projection algorithms with Shepp–Logan filtering. Threshold segmentation was performed for the segmentation of aligners from the background and teeth.

The scans were converted to Digital Imaging and Communications in Medicine format and analyzed using 3D computed tomography evaluation software (InVivo 6, Anatomage Inc., San Jose, CA, USA). Embrasure aligner gap and thickness were measured at the coronal and cervical levels on the labial/buccal and palatal sides of the central–lateral incisors, canine–first premolar, and second premolar–first molar (Fig. 2). To establish the axial measurement plane, sagittal planes were first defined for the central incisor, canine, and second premolar as follows: (1) for the central incisor and canine, the plane passed through the mesiodistal midpoint of the incisal edge or cusp tip and was oriented perpendicular to the incisal edge or mesiodistal cuspal line; (2) for the second premolar, the plane passed through the buccal and palatal cusp tips and was oriented perpendicular to the mesiodistal marginal ridge lines. The axial sections were then positioned perpendicular to each sagittal plane and parallel to the line connecting the labial and palatal CEJ points. The embrasure fit ratio was calculated based

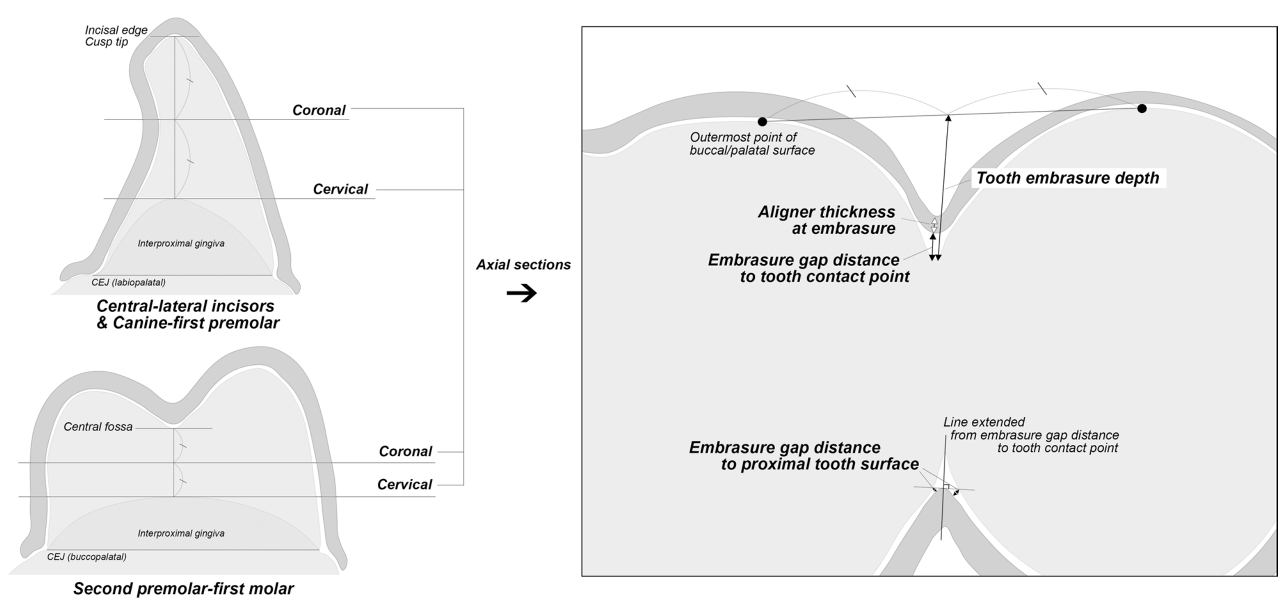

Fig. 2 Measurement of embrasure aligner gap distances and thickness at the vertical levels

on the gap distance relative to tooth embrasure depth. Aligner thicknesses at the embrasures were measured, and the ratio to the original sheet thickness or digital set value was also determined.

Statistical analysis

All measurements were performed by a single examiner (Dr. Ho-Jin Kim). Intra-examiner reliability was evaluated by remeasuring 10 randomly selected specimens after 2 weeks. Method error, calculated using Dahlberg's formula, ranged from 0.03 to 0.10 mm, and intraclass correlation coefficients exceeding 0.90 indicated excellent reliability.

Data normality was assessed using the Kolmogorov–Smirnov test. For non-normally distributed data, intergroup comparisons were conducted using the Kruskal–Wallis and the Mann–Whitney U tests.

Results

Comparison of embrasure aligner gap distance between groups

The null hypothesis of this study was rejected. In the embrasure between the central and lateral incisors on the labial side, aligner gap distances to the tooth contact point at both vertical levels were significantly smaller in the 0.05-mm offset 3D-printed group (0.32 ± 0.10 mm) compared with the no-offset (0.50 ± 0.12 mm) and thermoformed (0.53 ± 0.19 mm) groups (Table 1). No significant differences were observed on the palatal side. The aligner gap distance to the proximal surface of each incisor did not differ significantly among the groups, except at the labial–coronal level of the lateral incisor.

In the embrasure between the canine and first premolar, the gap distance to the contact point in the 0.05-mm offset 3D-printed group (0.26–0.56 mm) was significantly smaller than the no-offset 3D-printed group (0.47–1.02 mm) and thermoformed group (0.53–0.90 mm) at both vertical levels and on the labial and palatal sides. The gap distance to the proximal tooth surface was also significantly smaller in the 0.05-mm offset group, except on the labial side of the first premolar and at the palatal–coronal level of the canine.

For the embrasure between the second premolar and first molar, the gap to the contact point in the 0.05-mm offset 3D-printed group (0.40–0.74 mm) was significantly smaller than in the no-offset 3D-printed group (0.86–1.66 mm) and thermoformed group (0.85–2.25 mm). In particular, the thermoformed aligners showed the largest mean gap (2.25 mm) at the palatal–cervical level. The gap distance to the proximal tooth surface was greater in the thermoformed group (0.09–0.11 mm) compared with both 3D-printed groups (0.03–0.09 mm).

Comparison of embrasure gap distance to tooth contact point between vertical levels and embrasure fit ratio relative to tooth embrasure depth

For the embrasures between the incisors and between the second premolar and first molar, the no-offset 3D-printed and thermoformed groups exhibited significantly greater aligner gap distances to the tooth contact point at the cervical level (1.28–2.25 mm) compared with the coronal level (0.50–1.14 mm), except on the palatal side of the incisors (Table 2). In contrast, the 0.05-mm offset 3D-printed group demonstrated no significant difference between the vertical levels on either labial or palatal sides.

Interestingly, for the embrasure between the canine and first premolar, all groups showed smaller gaps at the cervical level than at the coronal level, except on the labial side of the no-offset 3D-printed group. This observation might be attributed to the greater anatomical divergence of the canine–first premolar embrasure at the cervical level compared with the coronal level.

When assessing embrasure fit relative to tooth embrasure depth (embrasure fit ratio), the 0.05-mm offset 3D-printed group (73–93%) demonstrated superior fit compared with the no-offset 3D-printed group (58–86%) and thermoformed group (44–85%).

Comparison of embrasure aligner thickness between groups

Embrasure aligner thickness was significantly lower in the thermoformed group (0.32–0.66 mm) compared with both 3D-printed groups (1.13–2.43 mm) (Table 3). When expressed as a ratio to the original virtual design thickness (0.5 mm) or the thermoformed sheet thickness (0.75 mm), the 3D-printed aligners demonstrated substantially higher values (197–470%), whereas the thermoformed aligners demonstrated considerably lower ratios (36.5–88.5%).

Discussion

This study evaluated the aligner–tooth gap at buccal and palatal embrasures in 3D-printed and thermoformed aligners, an area that has received limited attention in prior research. Embrasure fit is likely crucial to the accuracy of tooth movement as it can directly influence the grip of the aligner on tooth surfaces.

The 0.05-mm offset 3D-printed aligners demonstrated superior embrasure adaptation compared with the no-offset 3D-printed and thermoformed groups, showing reductions of 0.9 to 1.5 mm at the cervical level of the molars. In contrast, the thermoformed group showed larger gaps, which were further exacerbated in areas with pronounced tooth undercuts. At the cervical embrasures of the incisors and molars, the aligner gaps were 0.8 to 1.1 mm larger than at the coronal embrasures,

Table 1 Comparison of embrasure aligner gap distances among aligner groups

(mm)	3D-printed with no-offset ($n=10$)	3D-printed with a 0.05-mm offset ($n=10$)	Thermoformed ($n=10$)	
Tooth embrasures	**Mean ± SD (95% CI)**	**Mean ± SD (95% CI)**	**Mean ± SD (95% CI)**	***P* value**
Central–Lateral incisors				
Labial–Coronal level				
To Tooth contact point	0.50 ± 0.12 (0.40–0.59)^{A}	0.32 ± 0.10 (0.24–0.39)^{B}	0.53 ± 0.19 (0.37–0.69)^{A}	0.010*
To Central incisor	0.11 ± 0.05 (0.06–0.15)	0.06 ± 0.02 (0.04–0.08)	0.09 ± 0.04 (0.06–0.12)	0.070
To Lateral incisor	0.10 ± 0.03 (0.07–0.12)^{A}	0.05 ± 0.02 (0.03–0.07)^{B}	0.08 ± 0.03 (0.06–0.11)^{AB}	0.008**
Labial–Cervical level				
To Tooth contact point	1.28 ± 0.43 (0.92–1.64)^{A}	0.45 ± 0.20 (0.30–0.60)^{B}	1.34 ± 0.29 (1.10–1.58)^{A}	< 0.001***
To Central incisor	0.12 ± 0.07 (0.06–0.18)	0.09 ± 0.05 (0.05–0.13)	0.13 ± 0.07 (0.07–0.19)	0.453
To Lateral incisor	0.15 ± 0.09 (0.08–0.22)	0.08 ± 0.03 (0.06–0.11)	0.12 ± 0.06 (0.07–0.17)	0.289
Palatal–Coronal level				
To Tooth contact point	0.26 ± 0.10 (0.18–0.34)	0.24 ± 0.06 (0.19–0.29)	0.29 ± 0.11 (0.20–0.38)	0.762
To Central incisor	0.05 ± 0.02 (0.04–0.06)	0.05 ± 0.02 (0.03–0.07)	0.06 ± 0.03 (0.03–0.08)	0.866
To Lateral incisor	0.06 ± 0.02 (0.04–0.08)	0.05 ± 0.02 (0.03–0.06)	0.06 ± 0.03 (0.03–0.08)	0.454
Palatal–Cervical level				
To Tooth contact point	0.42 ± 0.24 (0.22–0.63)	0.20 ± 0.17 (0.07–0.34)	0.30 ± 0.18 (0.15–0.44)	0.277
To Central incisor	0.11 ± 0.07 (0.05–0.17)	0.06 ± 0.02 (0.05–0.08)	0.10 ± 0.04 (0.06–0.13)	0.293
To Lateral incisor	0.09 ± 0.08 (0.02–0.16)	0.07 ± 0.03 (0.05–0.09)	0.10 ± 0.05 (0.06–0.15)	0.352
Canine–First premolar				
Labial–Coronal level				
To Tooth contact point	0.62 ± 0.15 (0.49–0.74)^{AB}	0.44 ± 0.15 (0.32–0.55)^{A}	0.90 ± 0.31 (0.68–1.16)^{B}	0.002**
To Canine	0.08 ± 0.02 (0.06–0.09)^{A}	0.04 ± 0.02 (0.03–0.05)^{B}	0.11 ± 0.04 (0.07–0.14)^{C}	0.001**
To First premolar	0.06 ± 0.03 (0.04–0.09)^{A}	0.07 ± 0.04 (0.04–0.11)^{A}	0.11 ± 0.03 (0.08–0.13)^{A}	0.045*
Labial–Cervical level				
To Tooth contact point	0.69 ± 0.20 (0.50–0.88)^{A}	0.26 ± 0.12 (0.17–0.36)^{B}	0.57 ± 0.26 (0.35–0.78)^{A}	0.003**
To Canine	0.06 ± 0.03 (0.04–0.09)^{A}	0.07 ± 0.02 (0.05–0.08)^{A}	0.17 ± 0.09 (0.10–0.25)^{B}	0.010*
To First premolar	0.15 ± 0.12 (0.04–0.25)	0.07 ± 0.03 (0.05–0.09)	0.15 ± 0.10 (0.06–0.23)	0.181
Palatal–Coronal level				
To Tooth contact point	1.02 ± 0.18 (0.87–1.17)^{A}	0.56 ± 0.20 (0.41–0.71)^{B}	0.90 ± 0.47 (0.50–1.29)^{AB}	0.005**
to Canine	0.13 ± 0.06 (0.08–0.17)	0.09 ± 0.03 (0.06–0.11)	0.13 ± 0.03 (0.10–0.16)	0.063
To First premolar	0.22 ± 0.08 (0.16–0.28)^{A}	0.05 ± 0.02 (0.03–0.07)^{B}	0.08 ± 0.03 (0.05–0.11)^{B}	<0.001***
Palatal–Cervical level				
To Tooth contact point	0.47 ± 0.22 (0.29–0.65)^{A}	0.21 ± 0.11 (0.13–0.29)^{B}	0.53 ± 0.26 (0.32–0.75)^{A}	0.004**
To Canine	0.05 ± 0.02 (0.04–0.07)^{A}	0.06 ± 0.05 (0.02–0.09)^{A}	0.12 ± 0.04 (0.08–0.15)^{B}	0.005**
To First premolar	0.04 ± 0.02 (0.03–0.06)^{A}	0.05 ± 0.04 (0.02–0.08)^{A}	0.12 ± 0.06 (0.07–0.16)^{B}	0.013*
Second premolar–First molar				
Buccal–Coronal level				
To Tooth contact point	0.86 ± 0.12 (0.76–0.96)^{A}	0.40 ± 0.15 (0.22–0.59)^{B}	0.85 ± 0.28 (0.62–1.08)^{A}	0.004**
To Second premolar	0.04 ± 0.02 (0.02–0.06)^{AB}	0.03 ± 0.01 (0.02–0.05)^{A}	0.09 ± 0.03 (0.06–0.12)^{B}	0.014*
To First molar	0.05 ± 0.02 (0.04–0.07)	0.06 ± 0.02 (0.03–0.08)	0.09 ± 0.04 (0.05–0.12)	0.115
Buccal–Cervical level				
To Tooth contact point	1.54 ± 0.44 (1.17–1.91)^{A}	0.41 ± 0.36 (-0.04–0.85)^{B}	1.68 ± 0.40 (1.34–2.01)^{A}	0.004**
To Second premolar	0.06 ± 0.01 (0.06–0.07)^{A}	0.06 ± 0.03 (0.03–0.10)^{AB}	0.11 ± 0.03 (0.08–0.13)^{B}	0.009**
To First molar	0.09 ± 0.02 (0.07–0.11)^{A}	0.05 ± 0.02 (0.03–0.07)^{B}	0.10 ± 0.03 (0.08–0.13)^{A}	0.006**
Palatal–Coronal level				
To Tooth contact point	1.11 ± 0.23 (0.92–1.30)^{A}	0.60 ± 0.18 (0.37–0.82)^{B}	1.14 ± 0.25 (0.94–1.35)^{A}	0.004**
To Second premolar	0.07 ± 0.05 (0.03–0.11)^{AB}	0.04 ± 0.01 (0.02–0.05)^{A}	0.10 ± 0.04 (0.07–0.13)^{B}	0.028*
To First molar	0.04 ± 0.02 (0.03–0.05)	0.05 ± 0.04 (0.00–0.10)	0.06 ± 0.03 (0.04–0.09)	0.106
Palatal–Cervical level				
To Tooth contact point	1.66 ± 0.41 (1.32–2.00)^{A}	0.74 ± 0.26 (0.42–1.06)^{B}	2.25 ± 0.36 (1.94–2.55)^{C}	0.001**

Table 1 (continued)

(mm)	3D-printed with no-offset ($n = 10$)	3D-printed with a 0.05-mm offset ($n = 10$)	Thermoformed ($n = 10$)	
Tooth embrasures	**Mean ± SD (95% CI)**	**Mean ± SD (95% CI)**	**Mean ± SD (95% CI)**	***P* value**
To Second premolar	0.05 ± 0.02 (0.03–0.07)^A	0.04 ± 0.02 (0.02–0.06)^A	0.11 ± 0.02 (0.09–0.13)^B	0.001**
To First molar	0.06 ± 0.03 (0.03–0.08)^A	0.04 ± 0.01 (0.03–0.05)^A	0.10 ± 0.02 (0.08–0.11)^B	0.004**

SD standard deviation, *CI* confidence interval

The Kruskal–Wallis test was for group comparisons (*$P < 0.05$, **$P < 0.01$, or ***$P < 0.001$)

Values in the same row with different superscript letters are significantly different at $P < 0.05$ based on the Kruskal–Wallis and Mann–Whitney U tests

resulting in lower fit ratios of 44–55%. This may be attributed to limitations inherent in the thermoforming process, where aligner adaptation deteriorates in narrow or highly undercut regions. Furthermore, the gap distances to proximal tooth surfaces were greater in the thermoformed group than in both 3D-printed groups, suggesting that thermoformed aligners produce a blunter inner surface projection into the embrasure space (Figs. 3 and 4). Consequently, the enlarged gap space between thermoformed aligners and tooth surfaces reduces contact along mesial and distal surfaces, concentrating fit primarily in the buccal and palatal areas. These reduced embrasure fits are consistent with previous studies that reported potential adverse effects of poor cervical adaptation associated with the thermoforming process [8, 9, 21]. Moreover, embrasure gap distances were greater in molars with more convergent embrasures due to their relatively square occlusal anatomy (Figs. 3 and 4, and 5). This finding indicates that thermoformed aligners may provide an even poorer fit in cases of severe misalignment and confined interproximal spaces, thereby compromising tooth movement accuracy and resultantly increasing the necessity of the attachments.

In contrast, 0.05 mm offset 3D-printed aligners exhibited embrasure gap distances ranging from 0.2 to 0.7 mm with smaller standard deviations than the other groups. Across different embrasures, the variation in gap distance remained within 0.5 mm, which was significantly lower than the 2.0 mm difference observed in the thermoformed aligners. In addition, the 0.05 mm offset group showed no significant differences in gap distance between vertical levels of the incisors and molars. This consistent embrasure fit, compared with the variability seen in thermoformed aligners, may improve the predictability of tooth movement. In the no-offset group, embrasure gaps were larger than those in the 0.05 mm offset group, with greater discrepancies at the cervical region than at the coronal region. This finding may be attributed to thickening of the inner aligner surface due to excess resin during printing or post-processing [22]. Based on the current results, the superior embrasure fit achieved with the 0.05 mm offset underscores the importance of incorporating an appropriate inner surface offset in digital design to optimize tooth adaptation in 3D-printed aligners.

Overall, the 0.05-mm offset 3D-printed aligners demonstrated superior fit and greater thickness at the embrasures compared with thermoformed aligners. Enhanced embrasure adaptation and adequate thickness are expected to improve the accuracy of tooth movements, such as rotation, mesiodistal translation, and extrusion. In particular, proper adaptation at the cervical embrasure can facilitate planned tooth movements by effectively generating counteracting moments (Fig. 6). This desirable force-to-moment ratio, which may benefit bodily movement, is likely supported by the increased thickness observed at the cervical embrasures [23, 24]. In contrast, thermoformed aligners generally require supplementary attachments to compensate for poor embrasure fit and to increase the predictability of tooth movement. Although embrasure aligner fit may influence the accuracy of clinically achievable tooth movements, direct evidence linking fit quality to actual tooth movement remains limited. To address this gap, future in vitro studies could incorporate mechanical sensors [24] to quantify the forces and moments generated by aligners with varying embrasure adaptations or employ finite element analysis [25] to simulate their biomechanical effects. Furthermore, randomized prospective clinical trials are needed to validate these findings and assess their clinical relevance.

Additionally, the shape-recovery properties of 3D-printed aligners may further enhance embrasure adaptation and help with easier insertion and removal, even in cases with severe embrasure undercuts [6, 14, 26].

When assessing aligner thickness at the embrasures, the 3D-printed aligners exhibited an increase of 230–480% relative to the digital design thickness of 0.5 mm, which was significantly greater than that observed in the thermoformed aligners. This increase may be attributed to the retention of excess resin, particularly in more convergent or narrower embrasures, such as the cervical regions of posterior teeth. In contrast, the thermoformed group exhibited significant reductions in thickness, except at the palatal–coronal levels of the anterior teeth, where values exceeded the original sheet thickness of 0.75 mm, likely due to the oblique orientation of the axial section used for measurement relative to the actual aligner thickness. Thinning of thermoformed aligners was most

Table 2 Comparison of embrasure gap distance to the tooth contact point between vertical levels and embrasure fit ratio relative to tooth embrasure depth

	Central –Lateral incisors			**Canine –First premolar**			**Second premolar –First molar**		
	Coronal level	**Cervical level**		**Coronal level**	**Cervical level**		**Coronal level**	**Cervical level**	
	Mean ± SD	**Mean ± SD**	***P* value**	**Mean ± SD**	**Mean ± SD**	***P* value**	**Mean ± SD**	**Mean ± SD**	***P* value**
Labial side									
Embrasure gap distance (mm, a)									
3D-printed (no-offset)	0.50 ± 0.12	1.28 ± 0.43	0.001**	0.62 ± 0.15	0.69 ± 0.20	0.613	0.86 ± 0.12	1.54 ± 0.44	< 0.001***
3D-printed (0.05-mm offset)	0.32 ± 0.10	0.45 ± 0.20	0.113	0.44 ± 0.15	0.26 ± 0.12	0.006**	0.40 ± 0.15	0.41 ± 0.36	1.000
Thermoformed	0.53 ± 0.19	1.34 ± 0.29	< 0.001***	0.90 ± 0.31	0.57 ± 0.26	0.028*	0.85 ± 0.28	1.68 ± 0.40	0.002**
Tooth embrasure depth (mm, b)	1.75	2.88		3.05	3.91		3.11	3.71	
Embrasure fit ratio [(b-a)/b × 100, %]									
3D-printed (no-offset)	71.61 ± 6.73	55.51 ± 15.07		79.80 ± 4.85	82.35 ± 5.16		72.31 ± 3.81	58.59 ± 11.97	
3D-printed (0.05-mm offset)	81.84 ± 5.60	84.38 ± 6.86		85.72 ± 4.91	93.27 ± 3.07		87.01 ± 4.84	89.06 ± 9.66	
Thermoformed	69.71 ± 10.72	53.47 ± 9.95		70.41 ± 10.03	85.55 ± 6.69		72.67 ± 8.89	54.82 ± 10.82	
Palatal side									
Embrasure gap distance (mm, a)									
3D-printed (no-offset)	0.26 ± 0.10	0.42 ± 0.24	0.065	1.02 ± 0.18	0.47 ± 0.22	0.001**	1.11 ± 0.23	1.66 ± 0.41	0.007**
3D-printed (0.05-mm offset)	0.24 ± 0.06	0.20 ± 0.17	0.387	0.56 ± 0.20	0.21 ± 0.11	< 0.001***	0.60 ± 0.18	0.74 ± 0.26	0.310
Thermoformed	0.29 ± 0.11	0.30 ± 0.18	0.959	0.90 ± 0.47	0.53 ± 0.26	0.083	1.14 ± 0.25	2.25 ± 0.36	< 0.001***
Tooth embrasure depth (mm, **b)**	0.90	1.20		3.60	3.10		4.04	4.01	
Embrasure fit ratio [(b-a)/b × 100, %]									
3D-printed (no-offset)	71.11 ± 11.05	64.69 ± 20.36		71.67 ± 4.88	86.27 ± 6.14		72.52 ± 5.76	58.67 ± 10.14	
3D-printed (0.05-mm offset)	73.46 ± 6.88	82.96 ± 14.33		84.51 ± 5.44	93.33 ± 3.54		85.25 ± 4.49	81.55 ± 6.49	
Thermoformed	67.36 ± 12.11	75.21 ± 14.61		75.14 ± 13.07	82.78 ± 8.39		71.69 ± 6.10	44.01 ± 9.10	

SD standard deviation, *CI* confidence interval

The Mann–Whitney U test was used to compare embrasure gap distances between vertical levels (*$P < 0.05$, **$P < 0.01$, or ***$P < 0.001$)

Table 3 Comparison of embrasure aligner thickness and its ratio relative to original values

	Embrasure aligner thickness (mm)				Ratio (%)		
	3D-printed (no-offset)	3D-printed (0.05-mm offset)	Thermoformed		3D-printed (no-offset)	3D-printed (0.05-mm offset)	Thermoformed
	Mean ± SD (95% CI)	Mean ± SD (95% CI)	Mean ± SD (95% CI)	*P* value	Mean ± SD	Mean ± SD	Mean ± SD
Central–Lateral incisors							
Labial Coronal	1.46 ± 0.11 (1.37–1.55)^{A}	1.34 ± 0.17 (1.22–1.47)^{A}	0.54 ± 0.08 (0.48–0.61)^{B}	< 0.001***	292.00 ± 21.57	268.89 ± 33.05	72.33 ± 10.12
Cervical	1.47 ± 0.36 (1.17–1.77)^{A}	1.75 ± 0.24 (1.57–1.93)^{A}	0.33 ± 0.08 (0.26–0.40)^{B}	< 0.001***	294.50 ± 71.39	350.00 ± 47.13	44.33 ± 11.26
Palatal Coronal	1.32 ± 0.03 (1.30–1.35)^{A}	1.15 ± 0.10 (1.07–1.23)^{B}	0.82 ± 0.05 (0.78–0.86)^{A}	< 0.00***	264.50 ± 6.57	230.67 ± 20.59	108.83 ± 6.49
Cervical	1.38 ± 0.36 (1.08–1.68)^{A}	1.35 ± 0.26 (1.15–1.54)^{A}	0.48 ± 0.12 (0.39–0.58)^{B}	0.001**	276.75 ± 71.68	269.11 ± 51.62	64.50 ± 15.63
Canine–first premolar							
Labial Coronal	1.28 ± 0.10 (1.20–1.37)^{A}	1.44 ± 0.21 (1.28–1.60)^{A}	0.45 ± 0.07 (0.40–0.51)^{B}	< 0.001***	256.50 ± 20.58	288.44 ± 41.23	60.67 ± 9.40
Cervical	1.13 ± 0.21 (0.93–1.32)^{A}	1.39 ± 0.35 (1.12–1.66)^{A}	0.27 ± 0.08 (0.21–0.34)^{B}	< 0.001***	197.25 ± 88.69	278.00 ± 69.35	36.50 ± 10.57
Palatal Coronal	2.06 ± 0.09 (1.98–2.13)^{A}	2.29 ± 0.21 (2.14–2.45)^{A}	1.36 ± 0.20 (1.19–1.52)^{B}	< 0.001***	411.00 ± 17.27	458.89 ± 41.21	180.67 ± 26.80
Cervical	1.63 ± 0.19 (1.47–1.79)^{A}	1.64 ± 0.21 (1.47–1.80)^{A}	0.49 ± 0.10 (0.41–0.57)^{B}	< 0.001***	326.00 ± 37.48	327.11 ± 41.81	65.17 ± 13.34
Second premolar–first molar							
Buccal Coronal	1.29 ± 0.21 (1.11–1.46)^{A}	1.57 ± 0.28 (1.21–1.92)^{A}	0.28 ± 0.04 (0.25–0.32)^{B}	< 0.001***	257.00 ± 41.64	313.20 ± 56.60	37.83 ± 5.19
Cervical	1.65 ± 0.35 (1.35–1.94)^{A}	2.36 ± 0.25 (2.04–2.69)^{B}	0.32 ± 0.06 (0.27–0.37)^{C}	< 0.001***	329.00 ± 69.85	470.82 ± 52.76	42.67 ± 7.54
Palatal Coronal	1.83 ± 0.22 (1.65–2.02)^{A}	1.95 ± 0.22 (1.67–2.23)^{A}	0.66 ± 0.06 (0.61–0.72)^{B}	0.001**	366.50 ± 44.22	390.00 ± 44.72	88.50 ± 8.40
Cervical	1.93 ± 0.19 (1.78–2.09)^{A}	2.43 ± 0.38 (1.97–2.90)^{A}	0.63 ± 0.04 (0.59–0.66)^{B}	< 0.001***	386.50 ± 37.58	486.80 ± 75.53	83.83 ± 5.54

SD standard deviation, *CI* confidence interval

The Kruskal–Wallis test was used for group comparisons (*$P < 0.05$, **$P < 0.01$, or ***$P < 0.001$)

Values in the same row with different superscript letters are significantly different at $P < 0.05$ based on the Kruskal–Wallis and Mann–Whitney U tests

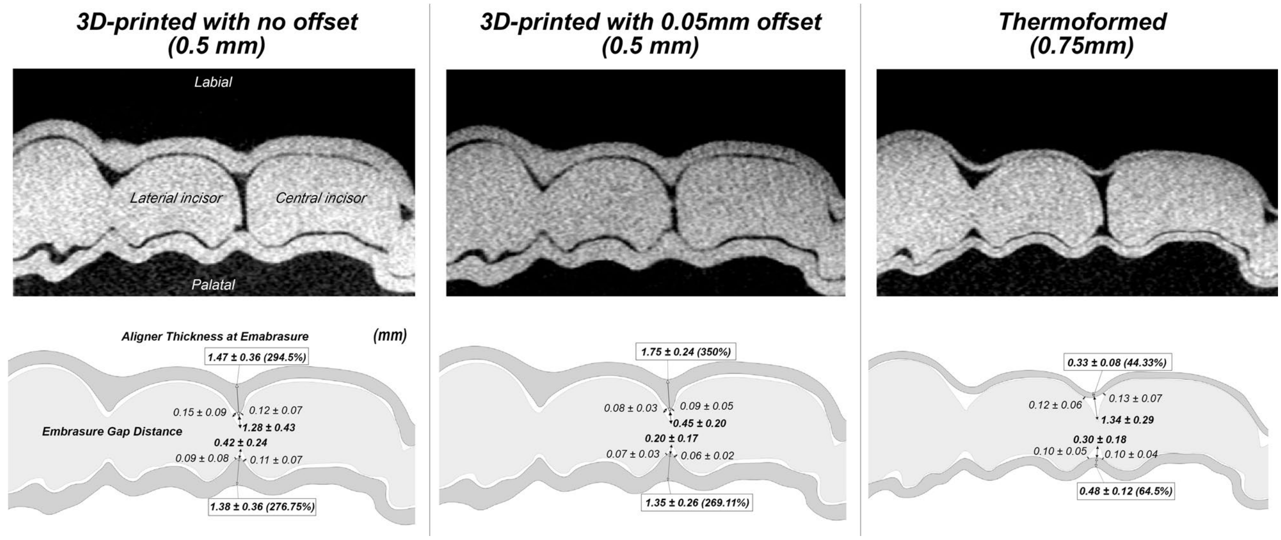

Fig. 3 Axial-sectioned microcomputed tomographic images of the cervical embrasures between central and lateral incisors, showing aligner gaps and thicknesses for each aligner group

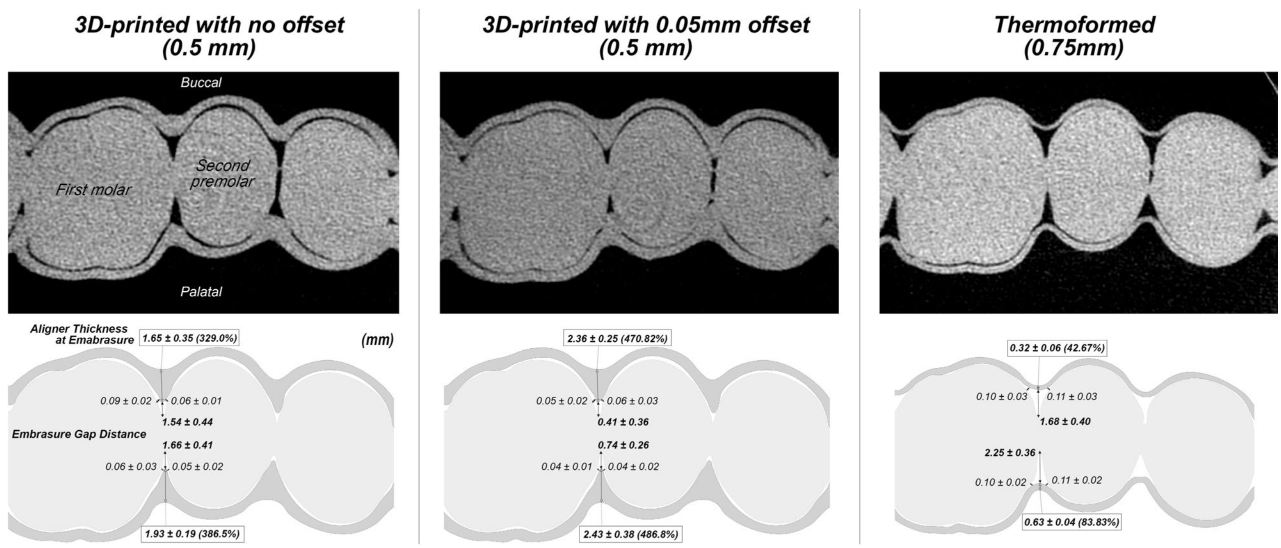

Fig. 4 Axial-sectioned microcomputed tomographic images of the cervical embrasures between the second premolar and first molar, showing aligner gaps and thicknesses for each aligner group

pronounced in areas with greater convergence or larger undercuts, such as the buccal sides of molars, and in the teeth with greater clinical crown height, such as the labiocervical regions of anterior teeth. These reductions in aligner thickness may compromise force delivery and result in inadequate control of tooth movements [22].

This study used a single maxillary dental model, and the aligners were fabricated with specific materials, trim lines, and post-processing protocols. These factors may limit the generalizability of the findings. Future research should include models with varying degrees of dental crowding and tooth inclination and employ diverse materials and fabrication methods to validate and broaden the applicability of the results.

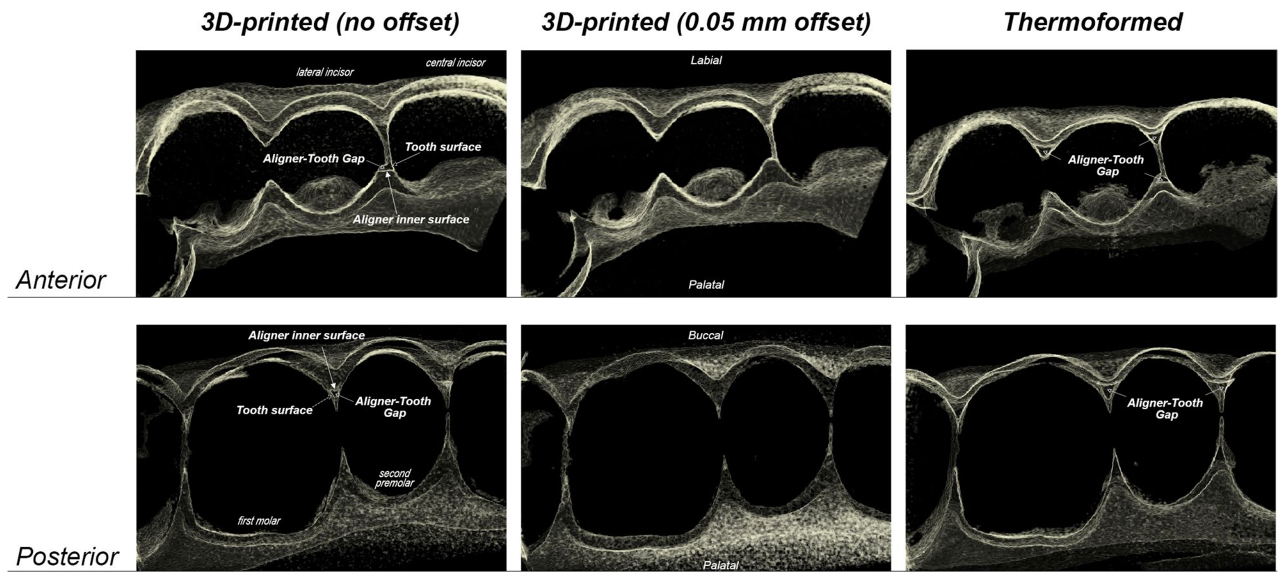

Fig. 5 Inverted three-dimensional microcomputed tomographic occlusal views of the cervical half region, showing aligner–tooth gaps at the embrasures

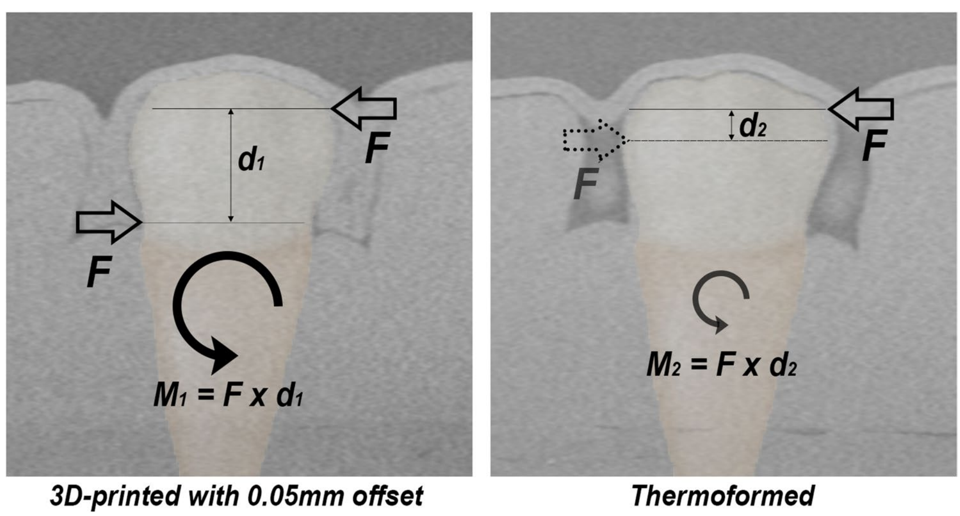

Fig. 6 Schematic illustration of the expected coupling moments in 3D-printed aligners with high embrasure fit ratios and thermoformed aligners with poor embrasure fit, based on mesiodistal sections from microcomputed tomography images

Conclusions

The 0.05 mm offset 3D-printed aligners showed smaller embrasure gap distances compared with the no-offset 3D-printed and thermoformed aligners.

The 3D-printed aligners demonstrated greater embrasure thickness ratios of 197–470% relative to the digital design thickness, while the thermoformed aligners exhibited reduced thickness ratios of 36.5–88.5% relative to the original sheet thickness.

Abbreviations

3D Three-dimensional
MicroCT Microcomputed tomography

Acknowledgements

Not applicable.

Author contributions

Dr. Ho-Jin Kim contributed to conceptualization, data curation, formal analysis, investigation, methodology, validation, visualization, original draft writing, and funding acquisition; Dr. Hyo-Sang Park contributed to conceptualization, methodology, supervision, validation, and manuscript review and editing. All authors have read and approved the final manuscript.

Funding

This work was supported by Kyungpook National University Dental Hospital Institute for Dental Research (2024).

Data availability

The data used and/or analysed during the current study are available from the corresponding author on reasonable request.

Declarations

Ethics approval and consent to participate
This study was approved by the appropriate institutional review board at Kyungpook National University Dental Hospital, Daegu, Korea (No.: KNUDH-2025-02-01-00).

Consent for publication
Not applicable.

Competing interests
The authors declare no competing interests.

Received: 18 October 2025 / Accepted: 16 December 2025
Published online: 29 December 2025

References
1. Haouili N, Kravitz ND, Vaid NR, Ferguson DJ, Makki L. Has invisalign improved? A prospective follow-up study on the efficacy of tooth movement with invisalign. Am J Orthod Dentofac Orthop. 2020;158:420–5.
2. Bilello G, Fazio M, Amato E, Crivello L, Galvano A, Currò G. Accuracy evaluation of orthodontic movements with aligners: a prospective observational study. Prog Orthod. 2022;23:12.
3. Kravitz ND, Kusnoto B, BeGole E, Obrez A, Agran B. How well does invisalign work? A prospective clinical study evaluating the efficacy of tooth movement with invisalign. Am J Orthod Dentofac Orthop. 2009;135:27–35.
4. Miao Z, Zhang H, Yang Y, Han Y, Leng J, Wang S. Influence of maxillary molar distalization with clear aligners on three-dimensional direction: molar distal movement, intrusion, distal tip and crown buccal torque. Prog Orthod. 2023;24:1.
5. Lombardo L, Palone M, Longo M, et al. MicroCT X-ray comparison of aligner gap and thickness of six brands of aligners: an in vitro study. Prog Orthod. 2020;21:12.
6. Upadhyay M, Arqub SA. Biomechanics of clear aligners: hidden truths and first principles. J World Fed Orthod. 2022;11:12–21.
7. Palone M, Longo M, Arveda N, et al. Micro-computed tomography evaluation of general trends in aligner thickness and gap width after thermoforming procedures involving six commercial clear aligners: an in vitro study. Korean J Orthod. 2021;51:135–41.
8. Hahn W, Zapf A, Dathe H, et al. Torquing an upper central incisor with aligners: acting forces and Biomechanical principles. Eur J Orthod. 2010;32:607–13.
9. Brezniak N. The clear plastic appliance: a Biomechanical point of view. Angle Orthod. 2008;78:381–2.
10. Castroflorio T, Sedran A, Parrini S, et al. Predictability of orthodontic tooth movement with aligners: effect of treatment design. Prog Orthod. 2023;24:2.
11. Kim DW, Lee HJ, Kim KB, et al. Force and moment analysis of clear aligners: impact of material properties and design on premolar rotation. Korean J Orthod. 2025;55:212–23.
12. Elshazly TM, Bourauel C, Ismail AM, et al. Effect of thermomechanical ageing on force transmission by orthodontic aligners made of different thermoformed materials: an experimental study. Orthod Craniofac Res. 2024;27:113–9.
13. Elshazly TM, Bourauel C, Ismail A, et al. Effect of material composition and thickness of orthodontic aligners on the transmission and distribution of forces: an in vitro study. Clin Oral Investig. 2024;28:258.
14. Lee SY, Kim H, Kim HJ, et al. Thermo-mechanical properties of 3D printed photocurable shape memory resin for clear aligners. Sci Rep. 2022;12:6246.
15. Panayi N, Cha JY, Kim KB. 3D printed aligners: material science, workflow and clinical applications. Semin Orthod. 2023;29:25–33.
16. Mantovani E, Castroflorio E, Rossini G, et al. Scanning electron microscopy evaluation of aligner fit on teeth. Angle Orthod. 2018;88:596–601.
17. Hisamitsu H, Iwaku M, Fusayama T. Measurements of cervical undercuts of human tooth crowns. J Dent Res. 1978;57:484–94.
18. Edelmann A, English JD, Chen SJ, Kasper FK. Analysis of the thickness of 3-dimensional-printed orthodontic aligners. Am J Orthod Dentofac Orthop. 2020;158:e91–8.
19. Cole D, Bencharit S, Carrico CK, Arias A, Tüfekçi E. Evaluation of fit for 3D-printed retainers compared with thermoform retainers. Am J Orthod Dentofac Orthop. 2019;155:592–9.
20. Park SY, Choi SH, Yu HS, et al. Comparison of translucency, thickness, and gap width of thermoformed and 3D-printed clear aligners using micro-CT and spectrophotometer. Sci Rep. 2023;13:10921.
21. Hahn W, Engelke B, Jung K, et al. Initial forces and moments delivered by removable thermoplastic appliances during rotation of an upper central incisor. Angle Orthod. 2010;80:239–46.
22. Hahn W, Dathe H, Fialka-Fricke J, et al. Influence of thermoplastic appliance thickness on the magnitude of force delivered to a maxillary central incisor during tipping. Am J Orthod Dentofac Orthop. 2009;136:e121–13.
23. Khalil AS, Zaher AR. Effect of printing orientation and resin thickness on flexural strength of direct 3D printed aligners. BMC Oral Health. 2025;25:238.
24. Grant J, Foley P, Bankhead B, Miranda G, Adel SM, Kim KB. Forces and moments generated by 3D direct printed clear aligners of varying labial and lingual thicknesses during lingual movement of maxillary central incisor: an in vitro study. Prog Orthod. 2023;24:23.
25. Inan A, Gonca M. Effects of aligner activation and power arm length and material on canine displacement and periodontal ligament stress: a finite element analysis. Prog Orthod. 2023;24:40.
26. Atta I, Bourauel C, Alkabani Y, et al. Physiochemical and mechanical characterisation of orthodontic 3D printed aligner material made of shape memory polymers (4D aligner material). J Mech Behav Biomed Mater. 2024;150:106337.

Publisher's note